Chinese Chemical Letters 34 (2023) 107469

Contents lists available at ScienceDirect

Chinese Chemical Letters

journal homepage: www.elsevier.com/locate/cclet

Characterization of two chimeric sesterterpene synthases from a fungal symbiont isolated from a sesterterpenoid-producing Lamiaceae plant *Leucosceptrum canum*

Desen Li[a,d,1], Minjie Yang[a,1], Rongfang Mu[a,d], Shihong Luo[c], Yuegui Chen[a,d], Wenyuan Li[a], An Wang[a], Kai Guo[b], Yan Liu[a,b,*], Shenghong Li[a,b,*]

[a] *State Key Laboratory of Phytochemistry and Plant Resources in West China, Kunming Institute of Botany, Chinese Academy of Sciences, Kunming 650201, China*

[b] *State Key Laboratory of Southwestern Chinese Medicine Resources, and Innovative Institute of Chinese Medicine and Pharmacy, Chengdu University of Traditional Chinese Medicine, Chengdu 611137, China*

[c] *College of Bioscience and Biotechnology, Shenyang Agricultural University, Shenyang 110866, China*

[d] *University of Chinese Academy of Sciences, Beijing 100049, China*

ARTICLE INFO

Article history:
Received 10 February 2022
Revised 22 April 2022
Accepted 24 April 2022
Available online 28 April 2022

Keywords:
Sesterterpenoids
Chimeric sesterterpene synthases
Plant symbiotic fungi
Alternaria alternata
Leucosceptrum canum
Anti-adipogenic activity

ABSTRACT

Two chimeric sesterterpene synthases (AaTPS1 and AaTPS2) were functionally characterized from *Alternaria alternata* MB-30 isolated from the leaves of a sesterterpenoid-producing Lamiaceae plant *Leucosceptrum canum*. AaTPS1 generated a 5/8/6/5 tetracyclic sesteraltererol **(1)** and its absolute stereochemistry was determined by X-ray crystallographic analysis of its derivative 10,11-epoxysesteraltererol **(2)**, which enabled revision of the absolute configuration of C7 of sesterfisherol produced by NfSS and PTTS014 characterized previously and its derivative 10,11-epoxysesterfisherol. AaTPS2 produced a 5/15 bicyclic preterpestacin I **(3)**. Site-directed mutagenesis suggested that F192 in AaTPS1 was likely involved in controlling of the hydroxylation of C12, and eight amino acids were important for the enzyme activity of AaTPS1 and AaTPS2. The engineered *Escherichia coli* and *Saccharomyces cerevisiae* strains were constructed for the productions of compounds **1** and **3**, and the highest titer of compound **1** reached 62.3 mg/L in shake-flask culture. Both compounds **1** and **2** showed anti-adipogenic activity.

Natural sesterterpenoids (C_{25}), a relatively unexplored subgroup of terpenoids with more than 1300 members characterized hitherto, have attracted intensive investigation recently due to their chemical complexity and biological diversity [1]. In addition to marine sponges producing approximately 65% of these compounds, sesterterpenoids are widely distributed in terrestrial fungi and plants, possessing complex cyclic skeletons and significant biological activities. The various sesterterpene skeletons are produced by sesterterpene synthases (sesterTPSs) from the linear precursor geranylfarnesyl diphosphate (GFDP). Fungal sesterTPSs are bifunctional chimeric enzymes containing a C-terminal prenytransferase (PT) domain and an N-terminal terpene cyclase (TC) domain [2], while sesterTPSs in plants and bacteria possess only a TC domain [1,3]. Most enzymatic products of sesterTPSs characterized to date contain a cyclopentane moiety, which is generated *via* either the type A (C_1-IV-V, cyclization between C_1-cation and the 4th and 5th olefins of GFDP) or type B (C_1-III-IV, cyclization between C_1-cation and the 3rd and 4th olefins of GFDP) cyclization route [2]. The majority of characterized sesterTPSs catalyze type A cyclization, producing stereochemically diverse sesterterpenoids *via* a common 5/15 bicyclic carbocation intermediate (Fig. S1 in Supporting information). The representative type A sesterTPS is *Neosartorya fischeri* sesterfisherol synthase (NfSS) producing sesterfisherol with a 5/6/8/5 tetracyclic ring system (Fig. 1), whose cyclization mechanism was investigated through isotopic labeling experiments and density functional theory calculations [4,5].

Our previous investigation on the chemistry, bioactivities and biosynthesis of sesterterpenoids led to the discovery of three unique families of sesterterpenoids with different frameworks (named leucosceptroids, colquhounoids and eurysoloids) from the Lamiaceae medicinal plants *Leucosceptrum canum*, *Colquhounia coccinea* var. *mollis* and *Eurysolen gracilis*, respectively [6–8]. These

* Corresponding authors at: State Key Laboratory of Phytochemistry and Plant Resources in West China, Kunming Institute of Botany, Chinese Academy of Sciences, Kunming 650201, China.

E-mail addresses: liuyan@cdutcm.edu.cn (Y. Liu), shli@mail.kib.ac.cn (S. Li).

[1] These authors contributed equally to this work.

https://doi.org/10.1016/j.cclet.2022.04.067
1001-8417/

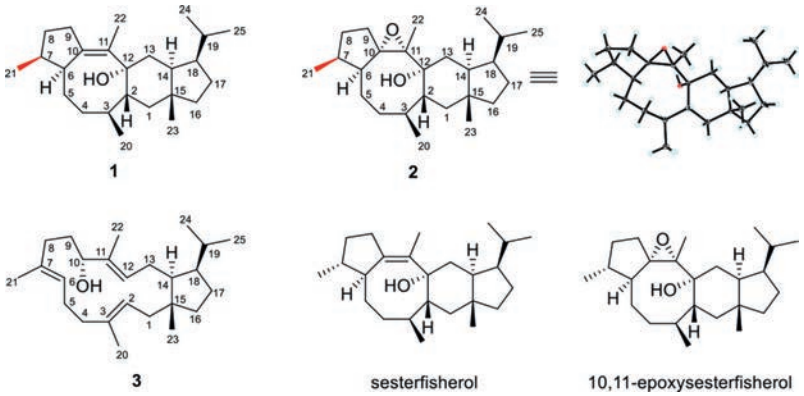

Fig. 1. Chemical structures of compounds **1–3**, sesterfisherol produced by NfSS and 10,11-epoxysesterfisherol.

compounds exhibited remarkable antifeedant, immunosuppressive and anti-adipogenic activities. Moreover, three enzymes involving in sesterterpenoid biosynthesis, including a GFDP synthase (GFDPS), a sester-/di-terpene cyclase (LcTPS2) producing 18-/14-membered macrocyclic terpenoids with immunosuppressive activity, and a promiscuous sester-/di-/sesqui-/mono-terpene synthase (CcTPS1), were identified from *L. canum* and *C. coccinea* var. *mollis* [9–11].

Endophytic fungi that have coevolved with higher plants are considered to be a promising producer of bioactive compounds [12–14], however the metabolic potential (especially sesterterpenoids) of fungal symbionts isolated from the above-mentioned three sesterterpenoid-producing plants remains largely uninvestigated. *Alternaria* species are the most widely existed plant endophytes and pathogens [15]. Recent phytochemical studies on *A. alternata* have identified three 5/15 bicyclic sesterterpenoids and a nitidasane sesterterpenoid sesteralterin with a 5/6/8/5 tetracyclic ring system, and some of them showed phytotoxic activity [16,17].

In this study, we describe the functional characterization of two chimeric sesterterpene synthases (AaTPS1 and AaTPS2) from a plant symbiotic fungus *A. alternata* MB-30 isolated from *L. canum* by their heterologous expressions in engineered *Escherichia coli* and *Saccharomyces cerevisiae*, respectively. AaTPS1 produces a 5/6/8/5 tetracyclic sesteraltererol **(1)** which could be converted to 10,11-epoxysesteraltererol **(2)** through non-enzymatic process while AaTPS2 generates the 5/15 bicyclic preterpestacin I **(3)**.

The endophytic fungus *A. alternata* MB-30 was isolated and identified from the leaves of *L. canum*. The genome of *A. alternata* SRC1lrK2f (BioProject: PRJNA239482) in public databases was used to search candidate sesterterpene synthases with the amino acid sequences of characterized fungal sesterTPSs (Table S1 in Supporting information). Two chimeric terpene synthases were found and designated as AaTPS1 and AaTPS2 (GenBank: XP_018386201 and XP_018380014). Phylogenetic analysis (Fig. S2 in Supporting information) showed that AaTPS1 and AaTPS2 fell within the clade of type A sesterTPSs that mainly generated bi-, tri-, and tetra-cyclic products with significant stereochemical diversity [2]. AaTPS1 was clustered with NfSS producing a tetracyclic sesterterpene, while AaTPS2 shared the highest homology with BaPS and BmTS3 that generated bicyclic sesterterpenes. Multiple sequence alignment of these two candidates with other fungal chimeric sesterTPSs (Fig. S3 in Supporting information) showed that both of them contain the typical "DDXXD" and "NSE/DTE" sequences in the TC domain and two aspartate-rich motifs "DDXXD" and "DDXXN" in the PT domain. These results suggested that AaTPS1 and AaTPS2 are typical chimeric terpene synthases and likely involved in the biosynthesis of polycyclic sesterterpenoids.

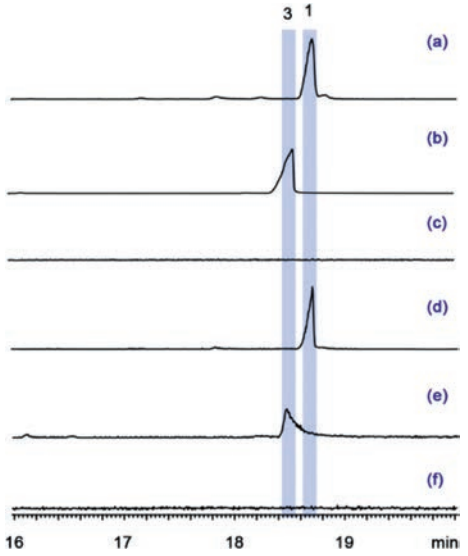

Fig. 2. GC–MS analysis (EIC: *m/z* 358) of the extracts of engineered *Escherichia coli* and *Saccharomyces cerevisiae* harboring AaTPS1 and AaTPS2. (a) AaTPS1 product in *E. coli*, (b) AaTPS2 product in *E. coli*, (c) the corresponding negative control in *E. coli*, (d) AaTPS1 product in *S. cerevisiae*, (e) AaTPS2 product in *S. cerevisiae*, (f) negative control in *S. cerevisiae*.

To characterize the function of AaTPS1 and AaTPS2, we attempted to amplify the full-length cDNA from mRNA of *A. alternata* MB-30 firstly. However, we failed to obtain *AaTPS1* cDNA using RT-PCR, presumably due to its low-level expression or even silencing. AaTPS1 gene contains two introns (Fig. S4 in Supporting information), and the full-length cDNA of AaTPS1 was then successfully obtained by overlap extension PCR using *A. alternata* MB-30 genomic DNA as the template. For heterologous expression in *E. coli*, the full-length cDNAs of AaTPS1 and AaTPS2 were then constructed into the vector pCold-TF generating pCold-TF/AaTPS1 and pCold-TF/AaTPS2, respectively. The recombinant vectors were individually transformed into the *E. coli* strains harboring the pBbA5c-MevT-MBIS plasmid that contained a complete gene set of the mevalonate (MVA) pathway and a farnesyl diphosphate (FDP) synthase gene [18]. Accordingly, the engineered *E. coli* strains EC-AaTPS1 and EC-AaTPS2 were constructed. GC–MS analysis showed that two peaks corresponding to compounds **1** and **3** with molecular ion peaks both at *m/z* 358 were produced by AaTPS1 and AaTPS2, respectively (Fig. 2 and Fig. S5 in Supporting information).

To illustrate the structures of compounds **1** and **3**, the *E. coli* strains harboring *AaTPS1/2* were cultured in a large scale, and the

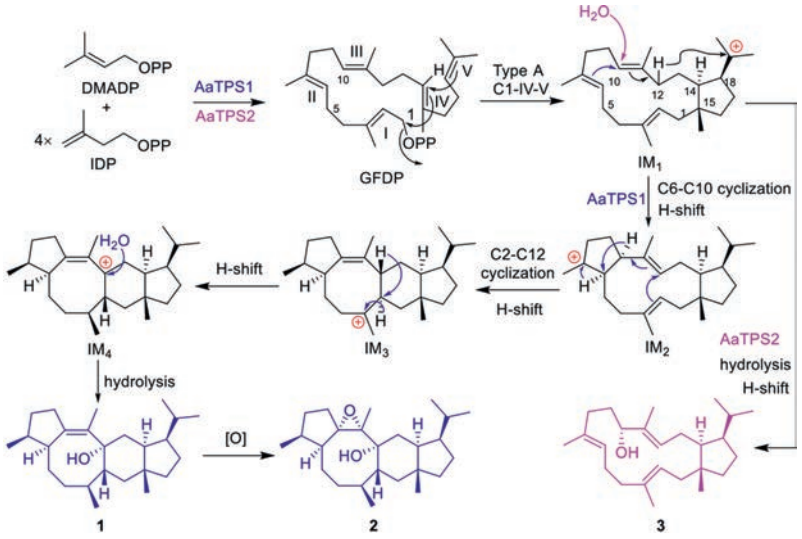

Fig. 3. Proposed cyclization mechanism of sesterterpenoids catalyzed by AaTPS1/2.

metabolites were extracted with petroleum ether and further purified with a combination of silica gel and sephadex LH-20 column chromatographies. Interestingly, compound **1** could be spontaneously converted to compound **2** during the separation process. Finally, we obtained adequate amounts of pure compounds **1**, **2** and **3** for further structural elucidation.

The characteristic ion fragments (*m/z* 69, 81, 340) and molecular ion peak at *m/z* 358 of compound **1** in GC–MS analysis suggested a sesterterpene for **1** (Fig. S5). ^{1}H and ^{13}C NMR spectra (Figs. S6–S13 in Supporting information) of **1** showed the presence of a double bond and an oxygenated quaternary carbon, however only 21 carbon signals could be observed and the remaining 4 signals were broadened, presumably due to slow conformational changes around the eight-membered ring according to the literature [4]. Despite, the ^{1}H and ^{13}C NMR spectral data of **1** were highly similar to those of sesterfisherol produced by NfSS and PTTS014 from *A. alternata* [4,19], suggesting that they might possess the same structure (Table S2 in Supporting information). Surprisingly, we found that **1** underwent oxidative transformation to generate a more polar compound **2** during the chromatographic purification with an $AgNO_3$-silica gel column. The ^{1}H and ^{13}C NMR data of **2** are almost identical with 10,11-epoxysesterfisherol, an oxidative product of sesterfisherol (Figs. S14–S19 and Table S3 in Supporting information). Fortunately, we obtained the single crystal of **2** after repeated crystallization in acetonitrile, which was submitted to X-ray crystallographic analysis for determination of its structure including absolute stereochemistry (Note S1, Fig. S20, Table S4 in Supporting information). Unexpectedly, the absolute configuration of C7 of **2** was different from that of 10,11-epoxysesterfisherol, while the other chiral carbons remained unchanged. C7 of **2** adopts *S* configuration according to the X-ray diffraction result, while in 10, 11-epoxysesterfisherol it was determined to be *R* by the vibrational circular dichroism (VCD) technique in conjunction with density functional theory (DFT) calculations [5]. Therefore, the structures of sesterfisherol and 10,11-epoxysesterfisherol should be revised as sesteralterol **(1)** and 10,11-epoxysesteralterol **(2)**, respectively. The ^{1}H and ^{13}C NMR spectra of **3** (Table S5 in Supporting information) showed the presence of 25 carbons including three double bonds and one oxygenated methine carbon, which was identified as preterpestacin I through careful comparison of its 1D and 2D NMR spectra (Figs. S21–S26 in Supporting information) and optical rotation ($[\alpha]_D^{20} = -27$) with the literature data [20,21]. However, since only relative configuration was deduced for preterpestacin I in the literature [20,21], **3** should have the same absolute configuration as **1** at C14, C15 and C18 from biogenetic consideration. The production of compounds **1** and **3** in engineered *E. coli* strains was then quantified by GC–MS method using the purified compounds as the external standards. It was found that the titers of compounds **1** and **3** in the engineered strains EC-AaTPS1 and EC-AaTPS2 were 5.07 mg/L and 1.38 mg/L under the shaking flask culture conditions, respectively (Fig. S27 in Supporting information).

To confirm the enzymatic products of AaTPS1 and AaTPS2 and further determine their yields in *S. cerevisiae*, the full-length cDNAs of AaTPS1 and AaTPS2 were constructed into the vector pESC-TRP, resulting in the recombinant pESC-TRP/AaTPS1 and pESC-TRP/AaTPS2, respectively. The 3–hydroxy-3-methylglutaryl coenzyme A reductase (HMG1) is a key rate-limiting enzyme in the MVA pathway and overexpression of a truncated HMG1 (tHMG1) could improve the production of isoprenoids [22]. Farnesyl diphosphate synthase (ERG20) could also increase the titer of FDP in engineered yeast [23]. Therefore, the plasmid pYX212-tHMG1-ERG20 was constructed and then co-transformed with pESC-TRP/AaTPS1/2 into the *S. cerevisiae* FY834 to generate the yeast strains SC-AaTPS1/2. After 96 h of shake-flask culture, the extracts were analyzed using GC–MS method. As we expected, the yeast strains harboring AaTPS1 and AaTPS2 could produce compounds **1** and **3**, respectively (Fig. 2). Quantitative analysis showed that the titer of compound **1** in the yeast strain SC-AaTPS1 reached 62.3 mg/L, which was approximately 12-fold higher than that in the *E. coil* strain EC-AaTPS1 (Fig. S27). The titer of compound **3** in SC-AaTPS2 was 1.07 mg/L, which was comparable to that in the *E. coil* strain.

Cyclization process catalyzed by AaTPS1 was proposed to be similar to that of NfSS reported previously Fig. 3 [4,5]. A common 5/15 carbocation intermediate **1** (IM_1) was generated *via* type A (C1-IV-V) cyclization. Subsequently, IM_1 underwent two successive C6-C10, C2-C12 cyclizations and H-shifts to generate intermediates IM_2, IM_3 and IM_4. IM_4 was then quenched by hydrolysis to give compound **1**. Compound **1** could be converted to **2** in a non-enzymatic oxidation process. For AaTPS2, IM_1 underwent H-shift and water-nucleophilic attack at C10 to generate the 5/15 bicyclic compound **3**.

To investigate the amino acid sites contributing to cyclization process and enzymatic activity, four candidate residues in AaTPS1 (L70, Y162, W166 and F192) and AaTPS2 (W69, F161, W165 and G191) at the corresponding positions were picked by careful analysis and alignment of their sequences (Fig. S2). Firstly, AaTPS1^{F192A}

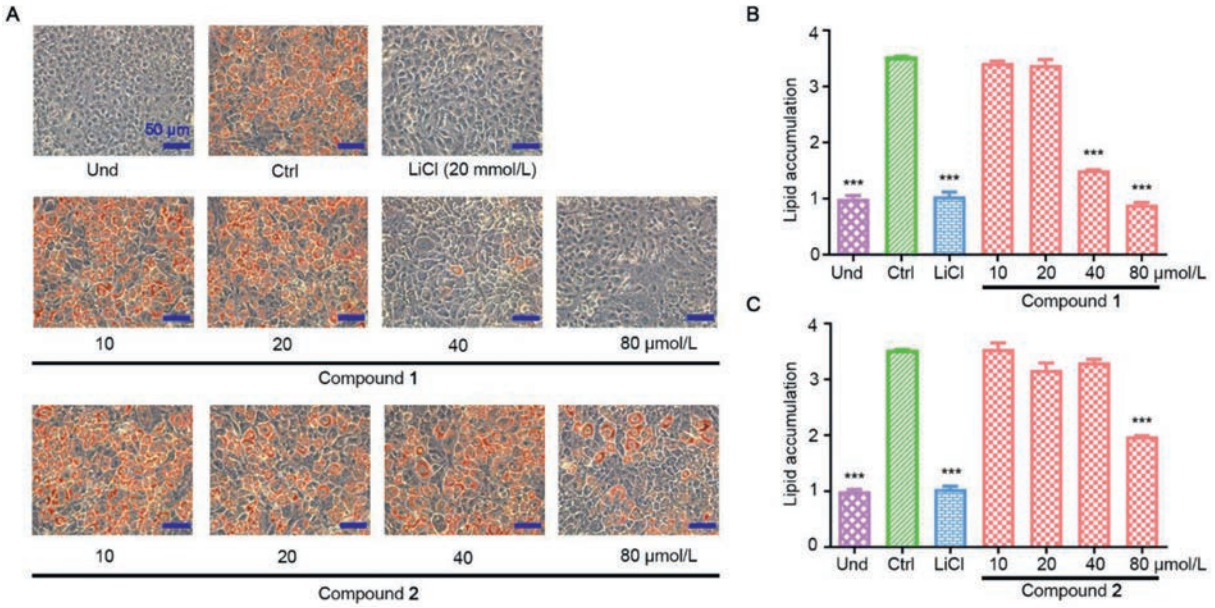

Fig. 4. Inhibitory effects of compounds **1** and **2** on lipid accumulation during 3T3-L1 adipocyte differentiation. (A) Representative images of cells treated with serial doses of compounds **1** and **2** and then stained with oil red O. (B) and (C) Normalized quantification of intracellular lipid contents treated with compound **1** (B) and compound **2** (C). Und, undifferentiated cells; Ctrl, fully differentiated cells used as negative control; LiCl (20 mmol/L), positive control.

and AaTPS2^{G191A} were constructed according to the docking simulation and site-directed mutagenesis analysis of NfSS reported previously [5]. GC–MS analysis showed that the *E. coli* harboring pBbA5c-MevT-MBIS and AaTPS1^{F192A} generated three new product peaks, besides compound **1** (Fig. S28 in Supporting information). Peaks 1 and 2 were presumably the products of IM_3 quenched by deprotonation at C1 or C20, and were tentatively identified as compounds **4** and **5**, respectively, based on their biogenesis with compound **1** in combination with a comparison of the fragmental patterns in their mass spectra with those reported in the literature [5]. Peak 3 should also be a sesterterpene with a similar structure, but to be characterized. Unfortunately, we have not obtained sufficient amount of samples of these compounds from the extract of *E. coli* harboring AaTPS1^{F192A} for NMR analysis due to their low yield and poor separation. In contrast, the activity of AaTPS2^{G191A} was reduced by approximately 56% and no deprotonated product was formed. In addition, eight variants (AaTPS1^{L70W}, AaTPS1^{Y162G}, AaTPS1^{W166G}, AaTPS1^{F192G}, AaTPS2^{W69L}, AaTPS2^{F161G}, AaTPS2^{W165G} and AaTPS2^{G191F}) were also constructed by swapping aromatic/nonaromatic residues. The production of compound **1** in variant AaTPS1^{Y162G} decreased by approximately 98%, while enzymatic activity of the other variants was completely lost (Fig. S28). These results indicated that F192 in AaTPS1 was likely involved in controlling of the hydroxylation of C12, and also highlighted the importance of the above residues for the enzyme activity.

The anti-adipogenic activity of compounds **1** and **2** were evaluated by measuring their inhibitory effect on lipid accumulation in 3T3-L1 adipocytes. The oil red O staining results showed that compound **1** inhibited the lipid content to 79.85% and 94.41% of the control at 40 and 80 μmol/L, respectively (Fig. 4). Compound **2** showed obvious inhibitory activity at 80 μmol/L, and the inhibition rate was 61.26% (Fig. 4). These results indicated that both compounds **1** and **2** showed antiadipogenic effect, but compound **2** with higher oxidation exhibited less potent activity.

In conclusion, we have functionally characterized two chimeric sesterterpene synthases AaTPS1 and AaTPS2 from *A. alternata* MB-30, a symbiotic fungus isolated from the leaves of *L. canum*. Their products were identified as a 5/8/6/5 tetracyclic sesterterpenoid sesteraltererol **(1)** and a 5/15 bicyclic sesterterpenoid preterpestacin I **(3)**, respectively. The absolute stereochemistry of **1** was determined by X-ray crystallographic analysis of 10,11-epoxysesteraltererol **(2)**, the non-enzymatic oxidation product of **1**, which allowed the revision of the reported structures of sesterfisherol produced by two chimeric sesterterpene synthases NfSS and PTTS014 characterized previously and its derivative 10,11-epoxysesterfisherol. Productions of compounds **1** and **3** in *E. coli* and *S. cerevisiae* were engineered, with the highest titer of 62.3 mg/L for compound **1** in shake-flask culture. The antiadipogenic activity of compounds **1** and **2** were observed.

Declaration of competing interest

The authors declare that they have no known competing financial interests or personal relationships that could have appeared to influence the work reported in this paper.

Acknowledgments

This work was supported financially by the National Natural Science Foundation of China (Nos. 21937006 and 22107103), the Yunnan Key Research and Development Program (No. 2019ZF011–2), and the “Western Light” Program of the CAS (to Y. Liu).

Supplementary materials

Supplementary material associated with this article can be found, in the online version, at doi:10.1016/j.cclet.2022.04.067.

References

[1] K. Guo, Y. Liu, S.H. Li, Nat. Prod. Rep. 38 (2021) 2293–2314.
[2] A. Minami, T. Ozaki, C. Liu, et al., Nat. Prod. Rep. 35 (2018) 1330–1346.
[3] A.W. Hou, J.S. Dickschat, Angew. Chem. Int. Ed. 59 (2020) 19961–19965.
[4] Y. Ye, A. Minami, A. Mandi, et al., J. Am. Chem. Soc. 137 (2015) 11846–11853.
[5] H. Sato, K. Narita, A. Minami, et al., Sci. Rep. 9 (2018) 2473.
[6] S.H. Luo, Q. Luo, X.M. Niu, et al., Angew. Chem. Int. Ed. 49 (2010) 4471–4475.
[7] C.H. Li, S.X. Jing, S.H. Luo, et al., Org. Lett. 15 (2013) 1694–1697.
[8] L.L. Teng, R.F. Mu, Y.C. Liu, et al., Org. Lett. 23 (2021) 2232–2237.
[9] Y. Liu, S.H. Luo, A. Schmidt, et al., Plant Cell 28 (2016) 804–822.
[10] Y.G. Chen, D.S. Li, Y. Ling, et al., Angew. Chem. Int. Ed. 60 (2021) 25468–25476.

[11] D.S. Li, J. Hua, S.H. Luo, et al., Plant Commun. 2 (2021) 100233.
[12] Y. Tan, Z. Guo, M. Zhu, et al., Chin. Chem. Lett. 31 (2020) 1406–1409.
[13] Y. Du, Z. Chen, H. Li, et al., Chin. Chem. Lett. 30 (2019) 981–984.
[14] P. Spiteller, Nat. Prod. Rep. 32 (2015) 971–993.
[15] B. Thomma, Mol. Plant Pathol. 4 (2003) 225–236.
[16] D.L. Guo, M. Zhao, S.J. Xiao, et al., Phytochem. Lett. 14 (2015) 260–264.
[17] Z.Z. Shi, F.P. Miao, S.T. Fang, et al., J. Nat. Prod. 80 (2017) 2524–2529.
[18] P.P. Peralta-Yahya, M. Ouellet, R. Chan, et al., Nat. Commun. 2 (2011) 483.
[19] R. Chen, Q.D. Jia, X. Mu, et al., Proc. Natl. Acad. Sci. U. S. A. 118 (2021) e2023247118.
[20] K. Narita, H. Sato, A. Minami, et al., Org. Lett. 19 (2017) 6696–6699.
[21] L. Jiang, G.L. Zhu, J.Y. Han, et al., Appl. Microbiol. Biotechnol. 105 (2021) 5407–5417.
[22] K.A.G. Donald, R.Y. Hampton, I.B. Fritz, Appl. Microbiol. Biotechnol. 63 (1997) 3341–3344.
[23] B.Y. Peng, M.R. Plan, P. Chrysanthopoulos, et al., Metab. Eng. 39 (2017) 209–219.